Resource Allocation Under Delay-Guarantee Constraints for Visible-Light Communication

FAN JIN, XUAN LI, RONG ZHANG, (Member, IEEE), CHEN DONG, AND LAJOS HANZO, (Fellow, IEEE)

School of Electronics and Computer Science, University of Southampton, Southampton SO17 1BJ, U.K.

Corresponding author: L. Hanzo (lh@ecs.soton.ac.uk)

ABSTRACT Visible light communications (VLCs) relying on commercially available light-emitting diode (LED) transmitters offer a huge data rate potential in this license-free spectral domain, while simultaneously satisfying energy-efficient conventional illumination demands. In an LED-based VLC system, the achievable data rate may be severely degraded owing to the interference, when the VLC system employs the unity frequency reuse (FR) approach. In order to mitigate the effects of interference, we propose a pair of interference avoidance approaches, namely, FR-based transmission and vectored transmission (VT). Furthermore, the resource allocation (RA) problems of indoor mobile terminals (MTs) are investigated based on different transmission strategies. Inspired by the concept of effective capacity (EC), we formulate our RA optimization problems applying proportional fairness, while satisfying specific statistical delay constraints. Our optimization procedure solves the RA problem of indoor MTs with the aid of a decentralized algorithm. Simulation results are also presented for quantifying the performance of the proposed algorithm. It is shown that both of our interference avoidance approaches are capable of reducing the interference, hence improving the overall performance. Furthermore, it is also observed that our VT transmission is capable of achieving a higher EC than the FR approach, when the statistical delay requirements are loose. By contrast, the FR-based transmission attains the best performance, when we tighten the delay requirements.

INDEX TERMS Resource allocation, transmission strategy, VLC system, effective capacity.

I. INTRODUCTION

Wireless access networks face an over-increasing data-rate requirement. However, the paucity of radio frequency (RF) bandwidth in the frequency ranges which facilitate a reasonable spatial coverage remains a limiting factor. As a result, alternative wireless transmission technologies have to be explored. With the promise of gaining access to a huge unlicensed bandwidth, which is available in the optical domain of the electromagnetic spectrum, the research of Optical Wireless (OW) communications intensified during the past decade or so [1]. Apart from the substantial amount of research on the infrared region of the optical spectrum [2], high data rate Visible Light Communication (VLC) combined with advanced illumination has become a reality in indoor scenarios [3]. Specifically, the Light-Emitting Diodes (LEDs) exhibit a high energy efficiency and, additionally, they are capable of exploiting a vast unregulated spectrum. Extensive investigations have been dedicated to the physical (PHY) layer of VLC [4]–[7].

In this paper, we consider an LED-based indoor VLC system, where the achievable downlink bit rate of indoor mobile terminals (MTs) is determined. The seminal study of [8] analysed the MTs' performance as a function of the received Signal to Noise Ratio (SNR) assuming that all LEDs in the room operate as a single transmission cell and activate a single LED light for downlink (DL) transmission according to the specific MT's position. Hence the resultant area spectral efficiency (ASE) of the LED light is low, since only a single MT is supported in a specific DL transmission slot. A straightforward technique of improving the ASE of the LED light is to simply transmit the DL signal simultaneously from every LED light. Hence each LED light creates a transmission cell. A major impairment imposed by this cell formulation is the interference between neighbouring LED lights. The performance of VLC systems is mainly dominated by the received Line-of-Sight (LoS) component, hence the more distant cell edge MTs may suffer from severe interference. In order to cope with this impairment, sophisticated transmission strategies have to be designed, but at the time of writing, there is a paucity of studies on the transmission strategies of VLC cells. The authors of [9] discussed Fractional Frequency Reuse (FFR) invoked for

VLC cells and subsequently a joint multi-LED transmission regime was derived in [10] and [11].

Apart from the transmission strategies designed for indoor VLC systems, another important issue of the indoor VLC architecture is its resource management mechanism. When multiple MTs are under the coverage of a single LED light, appropriate resource allocation (RA) schemes should be used for maintaining the Quality-of-Service (QoS) requirements. Future broadband wireless networks are expected to support a wide variety of communication services having diverse QoS requirements. Applications such as voice transmission as well as real-time lip-synchronized video streaming are delay-sensitive and they require a minimum guaranteed throughput. On the other hand, applications such as file transfer and email services are relatively delay-tolerant. As a result, it is important to consider the delay as a salient performance metric in addition to the classic physical layer performance metrics used for cross-layer optimization. Diverse approaches may be conceived for delay-aware resource control in wireless networks [12]–[18]. In order to satisfy the QoS requirements, we apply the *effective capacity* based approach of [12] for deriving the optimal RA algorithm, which guarantees meeting the statistical delay target of our indoor VLC system. A similar approach was employed in one of our previous contributions [19] in a hybrid VLC and femtocell system. However, our previous work considered the same transmission strategy as [8]. By contrast, in this paper, we address the optimal RA in the DL of a VLC system relying on different transmission strategies, while meeting both the bit rate and statistical delay targets of delay-sensitive traffic. The contributions of this paper are summarized as follows:

- We conceive an LED-based VLC system for providing indoor coverage. For a given position of the mobile terminal (MT), we assume a dispersive multipath channel, where the received optical power is constituted by the sum of the direct LOS optical power and of the first reflected optical power. Hence the resultant VLC channel has two different rates, a higher one for the non-blocked LOS channel-scenario, and a reduced rate in the blocked LOS channel-scenario, when only the reflected ray is received.

- In order to cope with the inter-cell interference of the VLC system considered, we employ a FR transmission approach, where the neighbouring LED lights employ a different frequency band.[1] In our novel Vectored Transmission (VT) approach, the neighbouring

two LED lights coordinate in order to perform Zero-Forcing (ZF) based beamforming (BF). We will show that both the proposed VT and BF approaches are capable of reducing the inter-cell interference.

- Limited-delay RA problems are formulated for both the FR and VT-aided the indoor VLC system. We then invoked the effective capacity approach of [12] for converting the statistical delay constraints into equivalent average rate constraints. Our RA problem is formulated as a non-linear programming (NLP) problem. We show mathematically that this NLP problem is concave with respect to the RA matrix $\boldsymbol{\beta}$, which hence can be solved by convex optimization techniques, such as the barrier method of [20]. A distributed algorithm using the dual decomposition approach of [21] is proposed.

The paper is organized as follows. In Section II, we describe our system model, including the link characteristics, the transmission strategies and the effective capacity of the VLC system. The formulation of our RA problems and the proposed distributed algorithms are outlined in Section III. Finally, our performance results are provided in Section IV and our conclusions are offered in Section V.

II. SYSTEM MODEL

We consider a 2-dimensional (2D) indoor room model. The set of MTs located or roaming in the indoor region is denoted by $\mathcal{N} = \{1, \cdots, n, \cdots, N\}$. We assume that the N MTs are randomly distributed in the room. A typical 2D-indoor VLC system using LED lights is illustrated in Fig. 1, where the LED lights are uniformly distributed on the ceiling of the room. Similarly, the set of LED lights is denoted by $\mathcal{M} = \{1, \cdots, m, \cdots, M\}$.
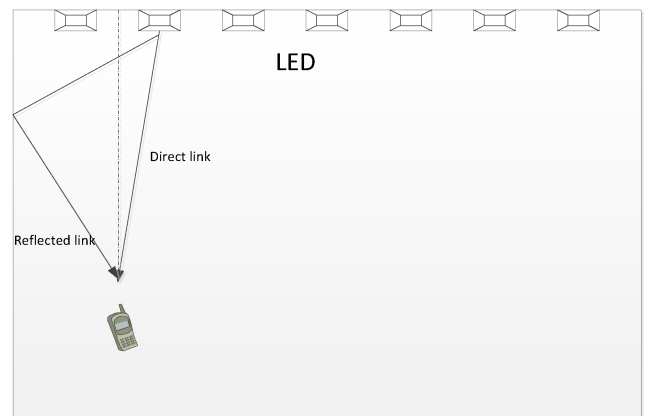

FIGURE 1. The 2D model of the room using the VLC system.

A. LINK CHARACTERISTICS

The propagation model of the VLC channel consists of the Line of Sight (LOS) path as well as the reflections of the walls in the room.[2] In this paper, the VLC channel is

---

[1]There are two popular techniques of constructing white LEDs, namely either by mixing the Red-Green-Blue frequencies using three chips, or by using a single blue LED chip with a phosphor layer. We consider the latter one, which is the favoured commercial version. Although the terminology of 'white' LED gives the impression of having all frequency components across the entire visible light spectrum, in fact only the blue frequency-range is detected. In fact, not even the entire blue frequency-range is detected, since the less responsive phosphorescent portion of the frequency-band is ignored. Hence, the modulation bandwidth is typically around 20 MHz, albeit this measured bandwidth depends on specific LED product used. Given this 20 MHz bandwidth, we are now ready to employ ACO/DCO-OFDM and partition it into arbitrary frequency reuse patterns.

[2]It is shown in [8] that the sum power of the reflected path is dominated by the first-reflection path. Hence, we also only consider the first-reflection path in our paper.

characterized by the LOS path plus a single primary reflected path.

Let us assume that ψ_{ir} is the angle of irradiation of the LED lights, ψ_{in} is the angle of incidence, while D_d is the distance between the transmitter and receiver. In an optical link, the channel's direct current (DC) gain H^d on the direct LOS path is given by [22]:

$$H^d = \begin{cases} \dfrac{(l+1)AT_s\kappa}{2\pi D_d^2}\mathcal{G}, & \text{if } \psi_{in} \leq \Psi_c, \\ 0, & \text{if } \psi_{in} > \Psi_c, \end{cases} \quad (1)$$

where l is the order of Lambertian emission, which is given by the semi-angle $\phi_{1/2}$ at half illumination of an LED as $l = \frac{\ln 2}{\ln(\cos\phi_{1/2})}$. Furthermore, A is the physical area of the photo-detector (PD), T_s is the gain of the optical filter used, and Ψ_c denotes the width of the field of view (FOV) at the receiver. Eq. (1) indicates that once the angle of irradiation of a receiver is higher than the Field of View (FOV), the receiver's LOS would be blocked. We assume that $\mathcal{G} = \cos^l(\psi_{ir})g(\psi_{in})\cos(\psi_{in})$, where $g(\psi_{in})$ is the gain of an optical concentrator [8], which can be characterized as [2]:

$$g(\psi_{in}) = \begin{cases} \dfrac{l^2}{\sin^2\Psi_c}, & \text{if } \psi_{in} \leq \Psi_c, \\ 0, & \text{if } \psi_{in} > \Psi_c. \end{cases} \quad (2)$$

Owing to the obstructions, the LOS propagation of the VLC system might be blocked. Here, we use the random variable κ to characterize the VLC LOS blocking events, which are assumed to be random. In line with [19], we assume that the event obeys the *Bernoulli distribution*, which indicates whether the VLC LOS reception is blocked or not. Its probability mass function may be expressed as:

$$f(\kappa) = \begin{cases} 1-p, & \text{if } \kappa = 1 \\ p, & \text{if } \kappa = 0, \end{cases} \quad (3)$$

where p denotes the VLC LOS blocking probability.

Apart from the VLC LOS reception, the MTs also receive the VLC reflected path owing to the wall. The channel gain owing to the reflection consists of the sum of all the channel gains of the reflected path, which may be written as:

$$H^r = \int_{\text{walls}} dH^{ref}, \quad (4)$$

where dH^{ref} denotes the first reflection from a small area of the wall, which is given by [8]:

$$dH^{ref} = \begin{cases} \dfrac{(p+1)AT_s\rho}{2\pi^2 D_1^2 D_2^2}\mathcal{J}\mathcal{G}dA_{\text{wall}}, & \text{if } \psi_{in} \leq \Psi_c, \\ 0, & \text{if } \psi_{in} > \Psi_c, \end{cases} \quad (5)$$

where D_1 is the distance between an LED light and a reflecting surface, D_2 denotes the distance between a reflective point and a MT receiver, ρ is the reflectance factor, whilst dA_{wall} is a small reflective area. Furthermore, we assume that $\mathcal{J} = \cos(\omega_1)\cos(\omega_2)$, where ω_1 and ω_2 denote the angle of

irradiance to a reflective point and the angle of irradiance to a MT's receiver, respectively.

Based on the above discussions, the VLC channel gain $H_{m,n}$ of the link spanning from the mth LED light to MT n is expressed as: $H_{m,n} = H_{m,n}^d + H_{m,n}^r$. The VLC channel gain matrix H is constituted by $(M \times N)$ elements. Having received the optical radiation, the photodetector converts the optical signal into electronic current.

The dominant noise contribution is assumed to be the shot noise due to ambient light impinging from the windows. We also take thermal noise into account. Hence, the receiver filter's output contains Gaussian noise having a total variance of σ^2 given by the sum of contributions from both the shot noise and the thermal noise, which is expressed as:

$$\sigma^2 = \sigma_{\text{shot}}^2 + \sigma_{\text{thermal}}^2. \quad (6)$$

According to [8], the variance of shot noise σ_{shot}^2 is given by:

$$\sigma_{\text{shot}}^2 = 2q\varsigma P_r B + 2qI_{bg}I_1 B, \quad (7)$$

where q is the electronic charge and ς is the detector's responsivity. B is the equivalent noise bandwidth and I_{bg} is the background current induced by the background light. Furthermore, the variance of thermal noise is given by [8]:

$$\sigma_{thermal}^2 = \frac{8\pi\varrho T_K}{G}\eta AI_1 B^2 + \frac{16\pi^2\varrho T_k\Gamma}{g_m}\eta^2 A^2 I_2 B^3, \quad (8)$$

where ϱ is the Boltzmann's constant, T_K is the absolute temperature, G is the open-loop voltage gain, η is the fixed capacitance of the PD per unit area, Γ is the FET channel noise factor, and finally, g_m is the FET transconductance. The noise bandwidth factors I_1 and I_2 are constant experimental values. Here, we opt for the typical values used in the literature [2], [8], namely for $I_1 = 0.562$ and $I_2 = 0.0868$.

Let us now define the Signal to Interference plus Noise Ratio (SINR) as the aggregate electronic power of the received signal set $\mathcal{S}$ over the noise power in a bandwidth of B [MHz], plus the sum of the electronic power received from other optical sources in the interference set $\mathcal{I}$. We assume that the VLC system relies on M-PAM based transmission. According to [3], the relationship between the bit error ratio (BER) and SINR (γ) for M-PAM signals is approximated as:

$$\text{BER}_{\text{M-PAM}} \approx \frac{Z-1}{Z}\frac{2}{\log_2 Z}Q\left(\frac{\sqrt{\gamma/2}}{Z-1}\right), \quad (9)$$

where Z represents the number of constellation points. As a result, the maximum affordable Z value may be found for a given BER target. Then, the achievable bit rate r of our VLC system is given by:

$$r = B\log_2 Z. \quad (10)$$

TABLE 1. Notations and system parameters.

2D indoor scenario	
Length of room	20m
Height of room	3m
Number of indoor MT	10
Height of MT	0.85m
Number of MTs	20
BER target of MTs	10^{-5}
VLC System	
Height of LED	2.5 [m]
Power of LED	20 [w]
Semi-angle at half power	70 [deg.]
Width of the field of view	115, 120, 125 [deg.]
Detector physical area of a PD	1.0 [cm^2]
Refractive index of a lens at a PD	1.5
O/E conversion efficiency	0.53 [A/W]
Available bandwidth for VLC system	10 [MHz]
Reflectance factor	0.8
Electronic charge	1.6×10^{-19} [C]
Background current	5.1×10^{-3} [A]
Open-loop voltage gain	10
Fixed capacitance of the PD per unit area	1.12×10^{-6}
FET channel noise factor	1.5
FET transconductance	3×10^{-2}

FIGURE 2. The achievable bit rate distribution of our VLC system under UFR transmission.

B. TRANSMISSION STRATEGY

1) UNITY FREQUENCY REUSE

The most straightforward way of constructing a VLC cell is to simply assume that each VLC light illuminates an individual cell, which corresponds to adopting Unity Frequency Reuse (UFR) across all VLC cells. Hence, apart from receiving the desired signal, a MT may also suffer from the interference impinging from the neighbouring LED lights. Here we denote the cell set by $\mathcal{C} = \{1, \cdots, c, \cdots, C\}$, where the number of cells C equals to the LED lights M for UFR transmission. As a result, the received SINR $\gamma_{c,n}$ of MT n served by cell c is given by:

$$\gamma_{c,n} = \frac{(\xi P_t H_{c,n})^2}{\sigma^2 B + \xi^2 \sum_{c' \neq c} (P_t H_{c',n})^2}, \qquad (11)$$

where ξ [A/W] denotes the photodetector's responsivity. Then, the instantaneous transmission bit rate is given by Eq. (9) and Eq. (10).

Here each traffic cell may serve multiple MTs and the total resources of a cell are normalized to unity. Assuming that the resources allocated to the MT n in cell c are denoted as $\beta_{c,n}$,[3] the bit rate achieved by MT n becomes $\beta_{c,n} r_{c,n}$, where $r_{c,n}$ denotes the instantaneous transmission bit rate according to Eq. (10).

The distribution of the achievable bit rate of our VLC system using the parameters listed in Table 1 under UFR transmission is characterized in Fig. 2. Observe from Fig. 2 that there are some coverage holes or dead zones, owing to the interference emanating from the neighbouring cells. As a result, more sophisticated transmission strategies have to be

employed in order to eliminate the interference and hence to provide improved VLC coverage.

2) FREQUENCY REUSE AIDED TRANSMISSION

Following the traditional cellular design principle, Frequency Reuse (FR) aided transmission may be employed for reducing the inter-cell interference (ICI). Here we involve this classic idea in our VLC system, where the neighbouring LED lights use a different frequency band, forming a VLC system having a factor 2.[4] Similarly, each VLC light illuminates an individual cell, and the pair of cell sets $\mathcal{C}_1, \mathcal{C}_2$ are defined as: $\mathcal{C}_1 = \{1, 3, \cdots, c, \cdots, C-1\}$ if c is odd, while as $\mathcal{C}_2 = \{2, 4, \cdots, c, \cdots, C\}$ if c is even, where $C = M$ assuming M is even. The two cell sets employ a different frequency band, hence ICI is avoid between these two sets. The received SINR $\gamma_{c,n}$ of MT n served by cell $c \in \mathcal{C}_1$ is given by:

$$\gamma_{c,n} = \frac{(\xi P_t H_{c,n})^2}{\sigma^2 B/2 + \xi^2 \sum_{c' \in \mathcal{C}_1, c' \neq c} (P_t H_{c',n})^2}. \qquad (12)$$

Since the FR transmission regime partitions the whole band into two frequency bands, the achievable transmission rate r of the VLC system under the FR transmission regime is given by

$$r = \frac{B}{2} \log_2 Z. \qquad (13)$$

Again, the bit rate achieved for MT n is $\beta_{c,n} r_{c,n}$. Although the FR transmission regime is an appealingly simple solution, the system has to obey the classic trade-off between a reduced Bandwidth Efficiency (BE) and a reduced dead zone area. In fact, supporting mobility is the most grave problem associated with FR during VLC cell formation, since switching

---

[3]$\beta_{c,n}$ is a general form of resource, which could be time, power, spectrum, etc. However, our proposed resource allocation algorithm is a generic one, which can be readily extended to the specific form of resource.
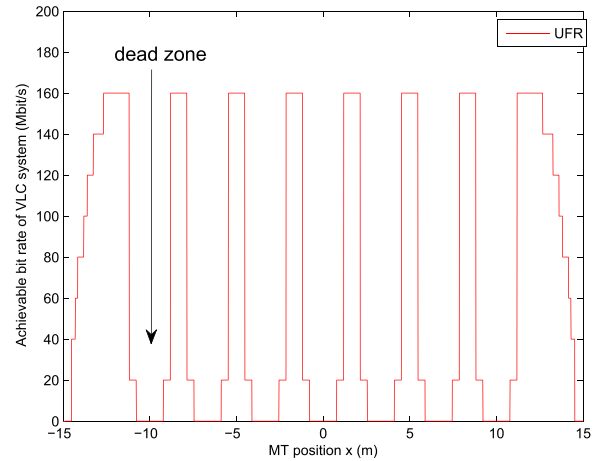
[4]In the 2-D indoor scenario considered, the ICI imposed by the direct link is completely avoided when employing a FR factor 2. We do not consider the FFR scheme, because FFR imposes a high complexity, and hence, it is unrealistic in VLC systems.

between frequencies every few meters during the MTs' movement degrades the users' quality of experience and this is why we do not consider the FFR based transmission strategy here [9].

3) VECTORED TRANSMISSION

In order to reduce the size of the ICI-infested area, whilst improving the mobility, several neighbouring LED lights can be merged into a virtual cell, where advanced transmission techniques may be employed in their overlapping areas. In this paper, the idea of Zero-Forcing (ZF) based vectored downlink transmission is employed in our VLC system model in order to eliminate the ICI, where the mutual interference between multiple users is completely eliminated by a beamforming matrix. Explicitly, we propose a transmission strategy,[5] where a pair of neighbouring LED lights constitute a virtual cell and perform ZF transmission. In the resultant VT regime, the cell set $\mathcal{C}$ is defined as $\mathcal{C} = \{1 \cdots c \cdots, C\}$, where $C = \frac{M}{2}$, assuming that M is even.

This VT-2 transmission regime is capable of simultaneously supporting transmissions in a specific frequency band for a maximum of two MTs. For a given served MT pair $\mathcal{P}_u = \{u_1, u_2\}$, the channel gain matrix $H_{c,\mathcal{P}_u}$ representing the transmissions from cell c to the MT pair $\mathcal{P}_u$ is denoted as $H_{c,\mathcal{P}_u} = [H_{c_1,u_1} H_{c_2,u_1}; H_{c_1,u_2} H_{c_2,u_2}]$, where c_1 and c_2 are the pair of LED lights in cell c, respectively. Then the resultant virtual cell is characterized by a weight matrix $G_{c,\mathcal{P}_u}$, which eliminates the interference between the MTs in $\mathcal{P}_u$ so that we have $H_{c,\mathcal{P}_u} G_{c,\mathcal{P}_u} = I^{2 \times 2}$, where I is the identity matrix. The matrix $G_{c,\mathcal{P}_u}$ can be readily derived by the pseudo-inverse of $H_{c,\mathcal{P}_u}$, which may be written by: $G_{c,\mathcal{P}_u} = H_{c,\mathcal{P}_u}^T \left(H_{c,\mathcal{P}_u} H_{c,\mathcal{P}_u}^T \right)^{-1}$, where H^T denotes the transpose of H. Furthermore, a power-sharing matrix $\Omega_{c,\mathcal{P}_u}$ is also defined in order to enforce the per LED power constraint for the sake of maintaining the total original power. In this paper we employ the power allocation scheme proposed in [23], which may be expressed as:

$$\Omega_{c,\mathcal{P}_u} = \omega_{c,\mathcal{P}_u} I, \quad \omega_{c,\mathcal{P}_u} = \min_\alpha \left(\frac{1}{\| G_{c,\mathcal{P}_u}(\alpha, :) \|_F} \right), \quad (14)$$

where $G_{c,\mathcal{P}_u}(\alpha, :)$ is the αth row of $G_{c,\mathcal{P}_u}$. As a result, the SINR γ_{c,u_1} with respect to the virtual cell c to the MT u_1 in the transmission pair $\mathcal{P}_u$ is given by:

$$\gamma_{c,u_1} = \frac{(\xi P_t \omega)^2}{\sigma^2 B + \xi^2 \sum_{m' \in \mathcal{M}'} \left(P_t H_{m',u_1} \right)}, \quad (15)$$

where $\mathcal{M}'$ denotes the set of interfering LED lights. Again, the achievable transmission rate of the VLC system relying on the FR transmission regime is also given by Eq. (9) and Eq. (10).

---

[5]For practical reasons, we only consider the coordination of a pair of neighbouring LED lights, since involving more LED lights would increase the complexity of the system.

TABLE 2. MT selection algorithm for VT-2 transmission.

Input
The position of MTs and LED lights.
Initialization
Initialize the cell association matrix $A \in \mathbb{R}^{N \times C}$ to be zero matrix
Cell association stage:
For $n \in \mathcal{N}$
MT n find the nearest LED light $m^\star$
finds the virtual cell $c^\star$ containing LED light $m^\star$
marks $A(n, c^\star) = 1$
End for
Exhausting search stage:
For $c \in \mathcal{C}$
finds the MTs in its coverage: find $A(:, c) = 1$
determines the number of its serving MTs N_c
lists all possible sorting combination π_c
For each sorting combination
For each transmission group
derive the sum bit rate according to Eq. (15), (9) and (10)
End for
records the sum bit rate for this sorting combination
End for
finds the best sorting pattern, which achieves the highest rate
End for
Output
The MT groups for all cells

If the total number of MTs in the coverage of a virtual cell is higher than two, each cell should carry out a MT pairing process first. In this paper, we propose a two-stage MT pairing algorithm, relying on the *cell association stage* and on an *exhaustive search stage*. In the first stage, each MT measures its the distance to all LED lights and sets up a connection with the LED light at the shortest distance.[6] As a result, this MT is associated with the cell covered by the LED light assigned. After this stage, each cell becomes aware of the identity of the associated MTs. In the second stage, the MTs linked to a specific cell should be sorted into several groups in order to employ VT-2 aided transmission, where each group contains a pair of MTs for transmission. This sorting problem is solved by an exhaustive search in our paper. Assuming that N_c MTs are associated with cell c, cell c firstly selects two MTs from these N_c MTs as a pair. Then it continues by selecting another two MTs from the remaining $(N_c - 2)$ MTs as a pair. Each cell repeats the selection process, until all MTs have been selected and paired. The potential number of MT pairs to be considered by the sorting process π equals to $\frac{C_{N_c}^2 C_{N_c-2}^2 \cdots 1}{(\lfloor N_c/2 \rfloor)!}$, where $C_{(\cdot)}^{(\cdot)}$ represents the combination, $\lfloor \cdot \rfloor$ is the floor operation and ! is the factorial operation. After the exhaustive search, each cell chooses the best pairing pattern from all π legitimate combinations, namely, the one which provides the highest sum of the achievable bit rates. The corresponding MT pairing algorithm is summarized in Table 2.

According to the above-mentioned MT selection algorithm, the virtual transmission cell c may simultaneously serve several groups of MTs. Since the MTs in the same group

---

[6]In this paper, we assume that LED lights have the knownledge of the LED MTs' position and report the distance to each MT.

share the same resources, a transmission group is defined as a virtual MT. In the resource allocation problem, we still use $\mathcal{N} = \{1, \cdots, n, \cdots, N\}$ to denote the virtual MT set for our VT-2 transmission strategy. Again, the bit rate achieved for the virtual MT n in the virtual cell c is $\beta_{c,n} r_{c,n}$, where $r_{c,n}$ is the sum of the transmission rates in the MT group n.

C. EFFECTIVE CAPACITY

In next-generation networks, it is essential to consider a range of QoS metrics, such as the achievable data rate, the tolerable delay and the delay-violation probability. During the early 90's, statistical QoS guarantees have been extensively studied in the context of the effective bandwidth theory of [24]–[26]. Explicitly, this theory states that for a dynamic queueing system having stationary ergodic arrival and service processes, the probability of exceeding a certain queue length decays exponentially. Inspired by the effective bandwidth theory, the authors of [12] proposed a link-layer metric termed as the effective capacity, which characterizes the effect of delay on the system. Owing to its advantages, the effective capacity has been widely adopted [12]–[16] for studying the steady-state delay-target violation probability. According to [12], for a dynamic queueing system where the arrival and service processes are both stationary and ergodic, the probability that the queue length $D(t)$ at an instant t of a service exceeds the maximum tolerable delay bound $D_{\max}$ is given by:

$$\Pr\{D(t) \geq D_{\max}\} \approx \gamma(t) e^{-\theta D_{\max}}, \quad (16)$$

where $\gamma(t) = \Pr\{D(t) \geq 0\}$ is the probability that the transmission queuing buffer is non-empty at a randomly selected instant t. Note from Eq. (16) that $\theta \geq 0$ is a crucial parameter, directly characterizing the exponential decaying rate of the probability that the delay exceeds D_{max}. As a result, θ may be referred to as the delay-related QoS exponent of a connection.

The effective capacity may also be interpreted as the maximum constant packet-arrival rate that the system is capable of supporting, without violating a given delay-related QoS requirement indicated by the QoS exponent θ. For uncorrelated block-fading channels, where the service process is also uncorrelated, the effective capacity is defined as [12], [27]:

$$\Delta(\theta) = -\frac{1}{\theta} \ln \mathbb{E}\left[\exp\left(-\theta r\right)\right], \quad (17)$$

where $\mathbb{E}(\cdot)$ is the expectation operator and r denotes the throughput.

Again, the channel gain of our VLC system is composed by the channel gain of the LOS path and that of the reflected path. In our paper, we assume that the LOS path may be blocked owing to the obstructions. As a result, the instantaneous transmission rate $r_{c,n}$ for a (virtual) MT n in (virtual) cell c obeys a Bernoulli distribution, with the probability mass function of:

$$f(r_{c,n}) = \begin{cases} 1 - p, & \text{if } r_{c,n} = \mathcal{R}_{1,n} \\ p, & \text{if } r_{c,n} = \mathcal{R}_{2,n}, \end{cases} \quad (18)$$

where $\mathcal{R}_{1,n}$ and $\mathcal{R}_{2,n}$ denote the achievable transmission rate of the VLC system to MT n both with and without VLC LOS

reception, respectively. As a result, the VLC transmission channel is modelled as a twin-rates channel.

Based on the above discussions, the VLC system's effective capacity, which is again the maximum constant packet-arrival rate that the service is capable of supporting under the statistical delay limit of the MT n specified by θ_n, may be expressed as:

$$\Delta_{c,n}\left(\beta_{c,n}\right) = \begin{cases} -\dfrac{1}{\theta_n} \ln \mathcal{Q}, & \text{if } \psi_{in} \leq \Psi_c \\ 0, & \text{if } \psi_{in} > \Psi_c, \end{cases} \quad (19)$$

where we have $\mathcal{Q} = p e^{-\theta_n \beta_{c,n} \mathcal{R}_{2,n}} + (1-p) e^{-\theta_n \beta_{c,n} \mathcal{R}_{1,n}}$.

III. PROBLEM FORMULATION AND SOLVING
A. PROBLEM FORMULATION

Our objective is to find the optimal RA per transmission cell by maximizing the sum of all MT's utility function. In this paper, the utility function $U_{c,n}\left(\beta_{c,n}\right)$ of MT n in cell c is defined as:

$$U_{c,n}\left(\beta_{c,n}\right) = \log\left[\Delta_{c,n}\left(\beta_{c,n}\right)\right], \quad (20)$$

where the logarithm is used here for guaranteeing fairness amongst the MTs served. As a result, the corresponding RA problem may be formulated as:

$$\text{Problem 1}: \underset{\boldsymbol{\beta}}{\text{maximize}} \sum_{c \in \mathcal{C}} \sum_{n \in \mathcal{N}} \log\left[\Delta_{c,n}\left(\beta_{c,n}\right)\right] \quad (21)$$

$$\text{subject to: } \sum_{n \in \mathcal{N}} \beta_{c,n} \leq 1, \quad \forall\, c \in \mathcal{C}, \quad (22)$$

$$0 \leq \beta_{c,n} \leq 1, \quad (23)$$

where $\boldsymbol{\beta}$ denotes the RA matrix of the VLC system. The effective capacity $\Delta_{c,n}$ of the VLC system is given by Eq. (19). Physically, the constraint (22) ensures that the total resources allocated in a cell always remain below unity. The constraint (23) describes the feasible region of the optimization variables.

B. DECENTRALIZED SUB-OPTIMAL RESOURCE ALLOCATION SCHEMES

Problem 1 described by Eq. (21), Eq. (22) and Eq. (23) may be solved with the aid of centralized optimization tools. However, in order to reduce the computational complexity and to make the problem tractable, in this section we propose decentralized sub-optimal RA schemes.

Since a (virtual) MT is always capable of connecting to a (virtual) cell, we may decouple Problem 1 into C number of subproblems. Each cell maximizes the sum of the logarithm of the MT's effective capacity. The subproblem for a specific traffic (virtual) cell c is formulated as:

$$\text{Problem 2}: \underset{\boldsymbol{\beta_c}}{\text{maximize}} \sum_{n \in \mathcal{N}_c} \log\left[\Delta_{c,n}\left(\beta_{c,n}\right)\right] \quad (24)$$

$$\text{subject to: } \sum_{n \in \mathcal{N}_c} \beta_{c,n} \leq 1, \quad (25)$$

$$0 \leq \beta_{c,n} \leq 1, \quad (26)$$

where $\boldsymbol{\beta}_c$ and $\mathcal{N}_c$ denote the RA vector of cell c and the MT set associated with cell c, respectively.

Lemma 1: The RA problem described by (24), (25) and (26) is a concave optimization problem.

Proof: See Appendix A. ∎

Since the problem is a concave one, convex duality implies that the optimal solution to this problem may be found with the aid of the Lagrangian formulation [20]. The Lagrangian function formulated for (24) under the constraints of (25) and (26) can be expressed as:

$$L\left(\boldsymbol{\beta}_c, \boldsymbol{\lambda}\right) = \sum_{n \in \mathcal{N}_c} \log\left[\Delta_{c,n}\left(\beta_{c,n}\right)\right]$$
$$- \sum_{n \in \mathcal{N}_c} \lambda_n \beta_{c,n} + \sum_{n \in \mathcal{N}_c} \lambda_n, \qquad (27)$$

where we have $\mathbf{0} \leq \boldsymbol{\beta}_c \leq \mathbf{1}$, while λ_n represents the Lagrange multipliers or prices associated with the nth inequality constraint (25). The dual objective function $g(\boldsymbol{\lambda})$ is defined as the maximum value of the Lagrangian over $\boldsymbol{\beta}_c$, which is expressed as:

$$g(\boldsymbol{\lambda}) = \sup_{\boldsymbol{\beta}_c} L\left(\boldsymbol{\beta}_c, \boldsymbol{\lambda}\right). \qquad (28)$$

The dual variable vector $\boldsymbol{\lambda}$ is dual feasible, if we have $\boldsymbol{\lambda} \geq 0$. The dual function can then be maximized for finding an upper bound on the optimal value of the original problem (24):

$$\min_{\boldsymbol{\lambda}} \ g(\boldsymbol{\lambda})$$
$$sub \ \boldsymbol{\lambda} \geq 0, \qquad (29)$$

which is always a convex optimization problem. The difference between the optimal primal objective and the optimal dual objective is referred to as the duality gap, which is always non-negative. A central result in convex analysis showed that when the problem is convex, the duality gap reduces to zero at the optimum [20], [28]. Hence, the primal problem of Eq. (24) can be equivalently solved by solving the dual problem of (29). In principle, the dual problem may be readily solved using standard routines, such as the Newton method and the barrier method [20]. However, these algorithms generally involve centralized computation and require global knowledge of all parameters. Hence, we propose an optimal decentralized RA algorithm for solving the problem using full dual decomposition [21]. Recall that in Eq. (28) we defined a dual objective function $g_n(\lambda_n)$ for MT n, which may be written as:

$$g_n(\lambda_n) = \log\left[\Delta_{c,n}\left(\beta_{c,n}\right)\right] - \lambda_n \beta_{c,n} + \lambda_n. \qquad (30)$$

Our primal problem described by (24), (25) and (26) may be separated into two levels of optimization. At the lower level, we decouple the problem of Eq. (28) into several sub-problems, where the nth subproblem may be written as:

$$\beta_{c,n}^{\star} = \underset{0 \leq \beta_{c,n} \leq 1}{\operatorname{argmax}} \ g_n(\lambda_n). \qquad (31)$$

It may be readily shown that $g_n(\lambda_n)$ is concave with respect to the variable $\beta_{c,n}$. Hence the maximization of $g_n(\lambda_n)$ may

be achieved by finding the partial derivative of $g_n(\lambda_n)$ with respect to $\beta_{c,n}$, which is given by:

$$\frac{\partial g_n(\lambda_n)}{\partial \beta_{c,n}} = \frac{\Delta_{c,n}'}{\Delta_{c,n}} - \lambda_n, \qquad (32)$$

where $\Delta_{c,n}' = \frac{d\Delta_{c,n}}{d\beta_{c,n}}$. Furthermore, the second partial derivative of $g_n(\lambda_n)$ is given by:

$$\frac{\partial^2 g_n(\lambda_n)}{\partial \beta_{c,n}^2} = \frac{\Delta_{c,n}'' \Delta_{c,n}}{\left(\Delta_{c,n}\right)^2} - \frac{\left(\Delta_{c,n}'\right)^2}{\left(\Delta_{c,n}\right)^2} \leq 0 \qquad (33)$$

As a result, $\frac{\partial g_n(\lambda_n)}{\partial \beta_{c,n}}$ is a monotonically decreasing function with respect to $\beta_{c,n}$. If we have $\left[\frac{\partial g_n(\lambda_n)}{\partial \beta_{c,n}} | \beta_{c,n} = 0\right] \leq 0$, then we may have $\beta_{c,n}^{\star} = 0$. If we have $\left[\frac{\partial g_n(\lambda_n)}{\partial \beta_{c,n}} | \beta_{c,n} = 1\right] \geq 0$, then we may have $\beta_{c,n}^{\star} = 1, \forall \ m$. Otherwise, $\beta_{c,n}^{\star}$ may be derived by solving the following Equation for a specific transmission cell c:

$$\frac{\Delta_{c,n}'}{\Delta_{c,n}} - \lambda_n = 0, \qquad (34)$$

which may be solved by the steepest descent method [20].[7]

At the higher level, we have the master dual problem, which may be expressed as:

$$\min_{\boldsymbol{\lambda}} g(\boldsymbol{\lambda}), \qquad (35)$$

where we have $g(\boldsymbol{\lambda}) = \sum_{n \in \mathcal{N}_c} g_{c,n}\left(\beta_{c,n}^{\star}, \lambda_n\right) + \sum_{n \in \mathcal{N}_c} \lambda_n$, and $\beta_{c,n}^{\star}$ denotes the optimal value derived from the lower level optimization problem of Eq. (31). Since the function $g(\boldsymbol{\lambda})$ is concave and differentiable, we can use a gradient method for solving the master dual problem, as a benefit of its simplicity. The derivative of $g(\boldsymbol{\lambda})$ with respect to $\boldsymbol{\lambda}$ is written as:

$$\frac{\partial g(\boldsymbol{\lambda})}{\partial \boldsymbol{\lambda}} = 1 - \sum_{n \in \mathcal{N}_c} \beta_{c,n}^{\star}. \qquad (36)$$

As a result, the price parameter $\boldsymbol{\lambda}$ is updated according to:

$$\lambda_n(t+1) = \left[\lambda_n(t) - \epsilon(t)\left(1 - \sum_{n \in \mathcal{N}_c} \beta_{c,n}^{\star}\right)\right]^{+}, \qquad (37)$$

where $[\cdot]^{+}$ is a projection on the positive orthant to account for the fact that we have $\lambda_m \geq 0$. Furthermore, $\epsilon(t)$ denotes the step-size taken in the direction of the negative gradient of the price parameter $\boldsymbol{\lambda}$ at iteration t. In order to guarantee convergence, where we have to satisfy $\lim_{t \to \infty} \epsilon(t) = 0$ and $\sum_{t=0}^{\infty} \epsilon(t) = \infty$. In this paper, we set $\epsilon(t) = \epsilon t^{-\frac{1}{2}+\varepsilon}$, ϵ and ε are positive constants.

---

[7]Nonlinear equations can be solved by several numerical methods. However, due to the length limitation of our paper, we will not be able to present the steepest descent method here.

C. REMARKS

Based on the above discussions, our decentralized optimal RA scheme is constituted by an iterative algorithm, which determines the optimal RA in the DL of cell c to MT n based on the update of the price parameters λ_n over a number of iterations, until the optimal solution is found. Each of the traffic cells involved this technique separately. For a specific cell c, each MT associated with this cell is initialized to a feasible price value λ_n. Then, each MT broadcasts its price value to its serving cell. Then each MT calculates the optimal RA based on the price information (λ) and the optimal resource $\beta^\star_{c,n}$ allocated from cell c to MT n is derived during the last iteration. Each MT updates its price value λ_n based on the optimal RA. The MTs broadcast their new price values λ to their associated cells and the process continues, until the algorithm converges. The decentralized optimal RA algorithm is formally described in Table. 3.

**TABLE 3.** Decentralized algorithm for Problem 1.

| Algorithm 1 |
| --- |
| **Input** |
| θ_n: Delay requirement of each MT n $\forall n$ |
| **Initialization** |
| $t \leftarrow 1$ |
| step size: positive ϵ and ε |
| **While** t does not reach its maximum |
| $\quad$ **For each transmission cell** |
| $\quad\quad$ **For each MT** $n \in \mathcal{N}_c$ |
| $\quad\quad\quad$ Initialize the price value: $\boldsymbol{\lambda}(t) = \{\lambda_1(t), ..., \lambda_{N_c}(t)\} = \mathbf{0}$ |
| $\quad\quad\quad$ Each MT solves the problem presented in Eq. (31); |
| $\quad\quad\quad$ Price value λ_n updates according to Eq. (37) |
| $\quad\quad$ **End for** |
| $\quad$ **End for** |
| $\quad \xi \leftarrow \epsilon t^{-\frac{1}{2}+\varepsilon}$ |
| $\quad t \leftarrow t+1$ |
| **End** |
| **Output** $\boldsymbol{\beta}^\star(t)$ |

IV. RESULTS AND DISCUSSIONS

In this section, we present our numerical performance results for characterizing the proposed RA algorithms in the context of the indoor VLC system of Fig. 1. Again, the 'two-rate' transmission channel model is used for our VLC system. We assume that the MTs are randomly and uniformly distributed in the room and that they all experience the same delay exponents. Our main system parameters are summarised in Table 1.

A. CUMULATIVE DISTRIBUTION FUNCTION OF THE EFFECTIVE CAPACITY

Fig. 3 compares the Cumulative Distribution Function (CDF) of effective capacity for different transmission strategies, in conjunction with a half field of view $\Phi_c = 60°$, a statistical delay parameter $\theta = 0.01$ and a VLC blocking probability of $p = 0.1$. Observe from the figure that almost 40% of the MTs are unable to attain a non-zero transmission rate for the UFR transmission, owing to the interference imposed by the neighbouring LED lights. By contrast, equitable fairness
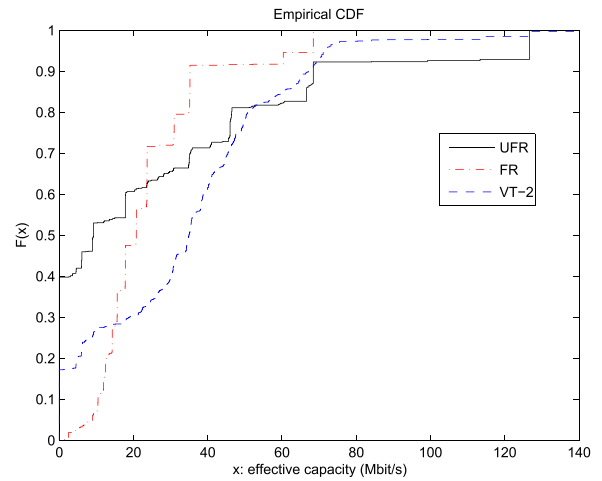
FIGURE 3. The CDF of effective capacity for different transmission strategies, with $\Phi_c = 60°$, $\theta = 0.01$, and $p = 0.1$.
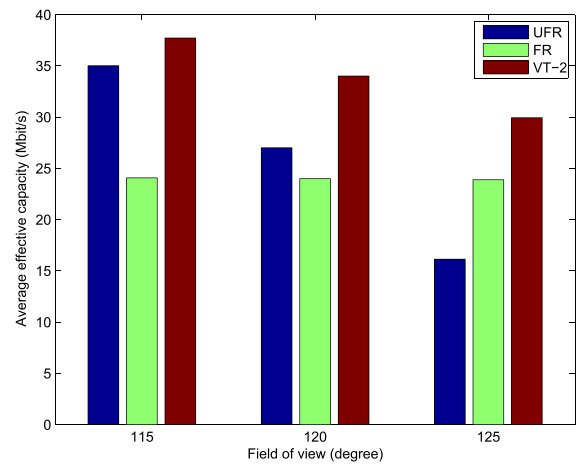
FIGURE 4. The average effective capacity of different transmission strategies versus the field of view of MTs, for $\theta = 0.01$ and $p = 0.1$.

is guaranteed under the FR transmission strategy, where all the MTs become capable of achieving a non-zero transmission rate. For our VT-2 transmission, about 20% of the MTs suffer from the dead-zone problem observed in Fig. 3. Although FR transmissions are capable of providing the most fair solution, the achievable rate of the 90% of the MTs ranges from 0 Mbit/s to 40 Mbit/s. By contrast, our VT-2 transmission is capable of providing a higher transmission rate.

B. EFFECT OF THE FIELD OF VIEW ANGLE

Increasing the FOV leads to the expansion of the areas contaminated by interference. As a result, the employment of interference reduction techniques may become more important. Fig. 4 demonstrates the relationship between the FOV and the average effective capacity of the MTs for the delay exponent of 0.01 and for the VLC LOS blocking probability of $p = 0.1$. Observe from Fig. 4 that the VLC system's effective capacity is reduced both for the UFR transmission

and for our VT-2 transmission, when we increase the FOV, because the increased interference erodes the attainable VLC performance. We also note that the performance of the UFR strategy is reduced more significantly than that of the VT-2 strategy, namely from 35 Mbit/s to 16Mbit/s for UFR transmission, and from 37 Mbit/s to 31Mbit/s for VT-2 transmission. The reason for this observation is that the interference is reduced by using our vectored transmission approach. By contrast, the average effective capacity remains unchanged, when the VLC system opts for FR transmission, since the interference is totally avoided when the neighbouring LEDs use a different frequency band. As a result, the FOV of the MTs does not unduly affect the received SINR. Furthermore, it is also shown that the highest average effective capacity is obtained by employing our VT-2 transmission in all the three scenarios considered.
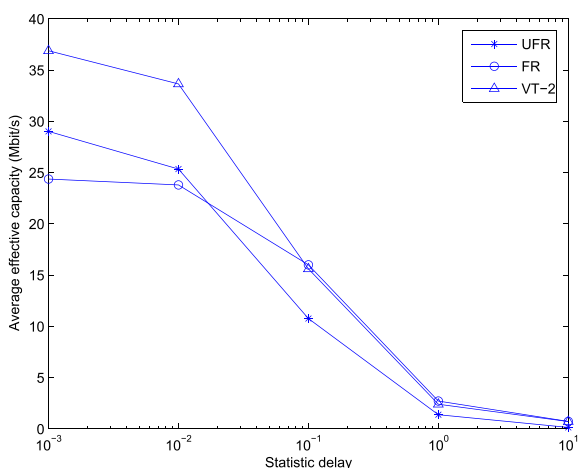

FIGURE 5. The average effective capacity of different transmission strategies versus the statistical delay parameter θ, for $\Phi_c = 60°$ and $p = 0.1$.

C. EFFECT OF THE DELAY STATISTICS

Fig. 5 illustrates the effect of the delay exponent θ on the average effective capacity of the MTs for the blocking probability $p = 0.1$. Observe from the figure that the average effective capacity is reduced upon increasing the delay exponent θ. However, the average effective capacity of the VLC system is fairly insensitive to the delay exponent, when the statistical delay exponent is relatively small. This is because when the delay exponent is low, the resultant delay requirement is loose and the effective capacity of the VLC system is close to the achievable rate, which depends on the wireless channel, but it is independent of the delay of the packet-arrival process. However, the average effective capacity degrades rapidly for $\theta \geq 0.01$. Furthermore, when the delay exponent is relatively high, the average effective capacity tends to zero. We also note from Fig. 5 that the proposed VT-2 transmission strategy obtains highest average effective capacity for $0.001 \leq \theta \leq 0.1$, while FR transmission may obtain a marginally higher average effective capacity for $\theta > 0.1$. This is because the VT-2 transmission outperforms the other

two transmission strategies, when the delay requirements is not too stringent. However, recal from Eq. (19) that the effective capacity is dominated by the first part of Eq. (19), when the resultant delay requirement becomes more tight, since $\mathcal{R}_{1,n}$ is much higher than $\mathcal{R}_{2,n}$. In other words, the MT's effective capacity is dominated by the reflected part of the LED light. As a result, FR may achieve the highest effective capacity, since there is no reflection-induced interference for FR transmissions.
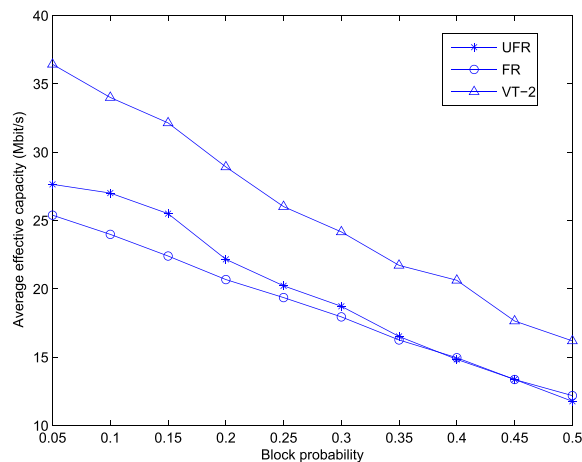

FIGURE 6. The average effective capacity of MTs versus the blocking probability of the VLC system p, for $\Phi_c = 60°$ and $\theta = 0.01$.
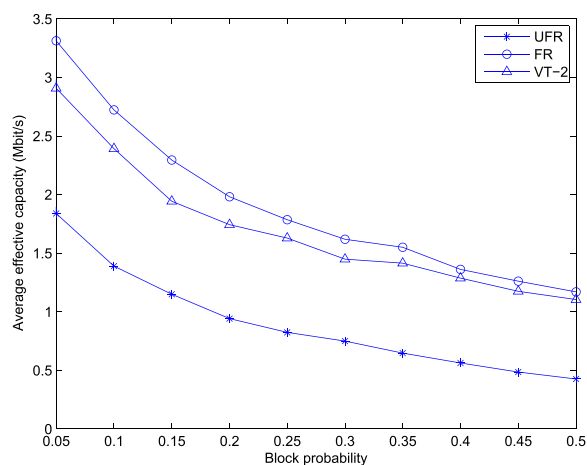

FIGURE 7. The average effective capacity of MTs versus the blocking probability of the VLC system, for $\Phi_c = 60°$ and $\theta = 1$.

D. EFFECT OF THE VLC SYSTEM's BLOCKING PROBABILITY

Let us now quantify the effect of the VLC system's blocking probability in Fig. 6 and Fig. 7 on the average effective capacity of the MTs, when using a delay exponent of 0.01 and 1, respectively. Firstly, we consider a loose delay requirement scenario. It is illustrated in Fig. 6 that the VLC system's average effective capacity is reduced,

when the blocking probability is increased. For the blocking probability considered, our VT-2 transmission is capable of achieving the highest effective capacity. We also note that UFR transmission is capable of achieving a higher effective capacity than FR transmission, when the blocking probability is below 0.35. When the LOS blocking probability of MTs is higher than 0.35, the FR transmission may achieve a higher effective capacity than UFR transmission, since the UFR performance is limited by the reflected path of the LED light.

Next, we consider a tight delay requirement scenario. In contrast to Fig. 6, we observe from Fig. 7 that FR transmission obtains the highest average effective capacity. Again, this is because the performance is dominated by the reflected part of the LED light in tight delay requirement scenarios, and FR transmission becomes the best for the reflection related transmission scenario. Hence, it is plausible that when MTs have tight delay requirements, both the FR transmission and the VT-2 transmission become more reliable.
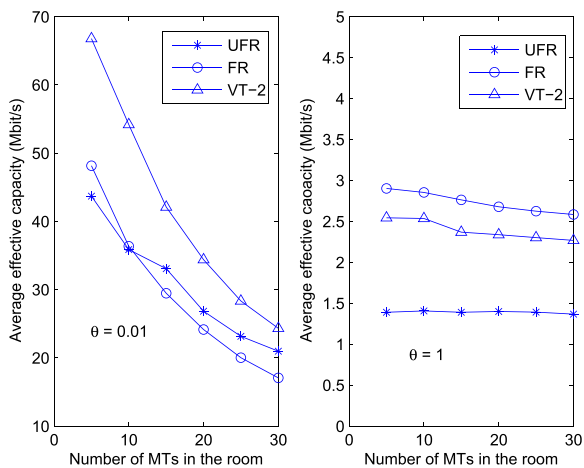

FIGURE 8. The average effective capacity of MTs versus the total number of MTs, for *p* = 0.1.

E. EFFECT OF THE TOTAL NUMBER OF MTs
Let us now quantify the effect of the total number of MTs on the VLC system's average effective capacity. Fig. 8 compares the overall effective capacity for different statistical delay requirements, when the number of MTs changes from 5 to 30. Since increasing the total number of MTs increases the load of each cell, the resources allocated to each MT are reduced, which results in the reduction of the average effective capacity, as shown in Fig. 8. For a loose delay requirement, our VT-2 transmission regime attains the best system performance, as expected. We also note that FR outperforms UFR transmissions, when the total number of MTs is less than 10. Recall from Fig. 3 that the dead zone area of UFR transmission is larger than that of FR transmission. When the number of MTs is low, it is more likely that no MT is located in the coverage of a cell and as a result, some of the resources may

be wasted by UFR transmission. When the number of MTs is increased, although the deadzone area of UFR transmission still remains wider than that of FR transmission, the VLC system's performance may not degrade too gravely, if there is at least one MT located in the transmission cell's coverage area. As a result, UFR transmission attains a better performance than UFR transmission in a denser scenario. However, when we have a tight statistical delay requirement, as illustrated at the right of Fig. 8, both the FR transmission and our VT-2 transmission regime obtain a similar performance, where FR transmission becomes even better than the VT-2 transmission. The reason for this is that the performance is dominated by the reflected path, when the delay requirements are tight. Hence we may conclude that our VT-2 transmission performs well in both the loose and tight delay scenario, albeit FR transmission outperforms it in a tight delay scenario.

V. CONCLUSIONS
In this paper, various VLC transmission strategies were investigated. We studied the classic frequency-reuse concept borrowed from cellular networks relying on FR in VLC environments as well as on our ZF-based coordinated transmission scheme. Furthermore, we studied the RA problems of mobile terminals (MTs) in a VLC system under diverse statistical delay requirements. The objective functions relied upon were shown to be concave. Furthermore, we proposed decentralized algorithms for solving the associated RA problem. The optimal RA for each iteration of the dual decomposition algorithm was presented and simulations were performed for validating the theoretical performance of the algorithm.

Finally, we compared the performance of various transmission strategies. The proposed FR and VT-2 transmission are capable of substantially reducing the interference and hence obtain a better performance than the traditional UFR transmission. However, these transmission strategies exhibit different system behaviours. FR transmission attains the best fairness, while our VT-2 transmission has a higher achievable bit rate. Furthermore, a comprehensive study of the effects of various system parameters was carried out. It is plausible that the VT-2 transmission is capable of achieving the highest effective capacity, when the statistical delay requirements are loose. However, FR transmission attains the best performance, when we tighten the delay requirements.

APPENDIX A
PROOF OF LEMMA 1
Firstly, we prove that the effective capacity $\Delta_{c,n}\left(\beta_{c,n}\right)$ of the link spanning from cell c of VLC system to MT n is a concave function of $\beta_{c,n}$. The first derivative of the effective capacity $\Delta_{c,n}\left(\beta_{c,n}\right)$ is given by:

$$\frac{d\Delta_{c,n}}{d\beta_{c,n}} = \frac{\mathcal{R}_{2,n}pe^{-\theta_n\mathcal{R}_{2,n}\beta_{c,n}} + \mathcal{R}_{1,n}\left(1-p\right)e^{-\theta_n\mathcal{R}_{1,n}\beta_{c,n}}}{pe^{-\theta_n\mathcal{R}_{2,n}\beta_{c,n}} + \left(1-p\right)e^{-\theta_n\mathcal{R}_n\beta_{c,n}}}.$$

(38)

Then the second derivative of the effective capacity $\Delta_{c,n}$ is given by:

$$\frac{d^2 \Delta_{c,n}}{d\beta_{c,n}^2} = -\frac{(\mathcal{R}_{1,n} - \mathcal{R}_{2,n})^2 \theta_n p (1-p) e^{-\theta_n \beta_{1,n}(\mathcal{R}_{1,n} + \mathcal{R}_{2,n})}}{\left[pe^{-\theta_n \mathcal{R}_{2,n}\beta_{c,n}} + (1-p) e^{-\theta_n \mathcal{R}_{1,n}\beta_{c,n}} \right]^2}$$
$$\leq 0, \quad \text{for } \theta_n \geq 0, \ 0 \leq p \leq 1. \quad (39)$$

Finally, the second derivative of $\log\left[\Delta_{c,n}\left(\beta_{c,n}\right)\right]$ with respect to $\beta_{c,n}$ may be written as:

$$\frac{d^2 \log\left[\Delta_{c,n}\left(\beta_{c,n}\right)\right]}{d\beta_{c,n}^2} = \frac{\Delta_{c,n}'' \Delta_{c,n}\left(\beta_{c,n}\right) - \left(\Delta_{c,n}'\right)^2}{\left(\Delta_{c,n}\right)^2}$$
$$\leq 0. \quad (40)$$

As a result, the objective function (24) of Problem 2 is a concave function with respect to $\beta_{c,n}$. The linear transformations of a concave function still constitute a function, hence the problem described by (24), (25) and (26) is a concave problem.

REFERENCES

[1] L. Hanzo, H. Haas, S. Imre, D. O'Brien, M. Rupp, and L. Gyongyosi, "Wireless myths, realities, and futures: From 3G/4G to optical and quantum wireless," *Proc. IEEE*, vol. 100, no. 5, pp. 1853–1888, May 2012.

[2] J. M. Kahn and J. R. Barry, "Wireless infrared communications," *Proc. IEEE*, vol. 85, no. 2, pp. 265–298, Feb. 1997.

[3] C.-L. Tsai and Z.-F. Xu, "Line-of-sight visible light communications with InGaN-based resonant cavity LEDs," *IEEE Photon. Technol. Lett.*, vol. 25, no. 18, pp. 1793–1796, Sep. 15, 2013.

[4] H. Le Minh *et al*, "100-Mb/s NRZ visible light communications using a postequalized white LED," *IEEE Photon. Technol. Lett.*, vol. 21, no. 15, pp. 1063–1065, Aug. 1, 2009.

[5] J. Armstrong, "OFDM for optical communications," *J. Lightw. Technol.*, vol. 27, no. 3, pp. 189–204, Feb. 1, 2009.

[6] R. Zhang and L. Hanzo, "Multi-layer modulation for intensity-modulated direct-detection optical OFDM," *IEEE/OSA J. Opt. Commun. Netw.*, vol. 5, no. 12, pp. 1402–1412, Dec. 2013.

[7] J. Jiang, R. Zhang and L. Hanzo, "Analysis and design of three stage concatenated color ShiDĚ Keying," *IEEE Trans. Veh. Technol.*, vol. 64, no. 11, pp. 5126–5136, Nov. 2015.

[8] T. Komine and M. Nakagawa, "Fundamental analysis for visible-light communication system using LED lights," *IEEE Trans. Consum. Electron.*, vol. 50, no. 1, pp. 100–107, Feb. 2004.

[9] C. Chen, N. Serafimovski, and H. Haas, "Fractional frequency reuse in optical wireless cellular networks," in *Proc. IEEE 24th Int. Symp. PIMRC*, London, U.K., Sep. 2012, pp. 3594–3598.

[10] C. Chen, D. Tsonev, and H. Haas, "Joint transmission in indoor visible light communication downlink cellular networks," in *Proc. IEEE Globecom Workshops*, Atlanta, GA, USA, Dec. 2013, pp. 1127–1132.

[11] X. Li, R. Zhang and L. Hanzo, "Coopera.ve load balancing in hybrid visible light communica.ons and WiFi," *IEEE Trans. Commun.*, vol. 63, no. 4, pp. 1319–1329, Apr. 2015.

[12] D. Wu and R. Negi, "Effective capacity: A wireless link model for support of quality of service," *IEEE Trans. Wireless Commun.*, vol. 2, no. 4, pp. 630–643, Jul. 2003.

[13] M. Tao, Y.-C. Liang, and F. Zhang, "Resource allocation for delay differentiated traffic in multiuser OFDM systems," *IEEE Trans. Wireless Commun.*, vol. 7, no. 6, pp. 2190–2201, Jun. 2008.

[14] D. S. W. Hui, V. K. N. Lau, and H. L. Wong, "Cross-layer design for OFDMA wireless systems with heterogeneous delay requirements," *IEEE Trans. Wireless Commun.*, vol. 6, no. 8, pp. 2872–2880, Aug. 2007.

[15] J. Tang and X. Zhang, "Cross-layer resource allocation over wireless relay networks for quality of service provisioning," *IEEE J. Sel. Areas Commun.*, vol. 25, no. 4, pp. 2318–2328, May 2007.

[16] Y. Cui, V. K. N. Lau, R. Wang, H. Huang, and S. Zhang, "A survey on delay-aware resource control for wireless systems—Large deviation theory, stochastic Lyapunov drift, and distributed stochastic learning," *IEEE Trans. Inf. Theory*, vol. 58, no. 3, pp. 1677–1701, Mar. 2012.

[17] N. McKeown, A. Mekkittikul, V. Anantharam, and J. Walrand, "Achieving 100% throughput in an input-queued switch," *IEEE Trans. Commun.*, vol. 47, no. 8, pp. 1260–1267, Aug. 1999.

[18] L. Tassiulas and A. Ephremides, "Dynamic server allocation to parallel queues with randomly varying connectivity," *IEEE Trans. Inf. Theory*, vol. 39, no. 2, pp. 466–478, Mar. 1999.

[19] F. Jin, R. Zhang, and L. Hanzo, "Resource allocation under delay-guarante constraints for heterogeneous visible-light and RF femtocell," *IEEE Trans. Wireless Commun.*, vol. 14, no. 2, pp. 1020–1034, Feb. 2015.

[20] S. Boyd and L. Vandenberghe, *Convex Optimization*. Cambridge, U.K.: Cambridge Univ. Press, 2004.

[21] M. Chiang, S. H. Low, A. R. Calderbank, and J. C. Doyle, "Layering as optimization decomposition: A mathematical theory of network architectures," *Proc. IEEE*, vol. 95, no. 1, pp. 255–312, Jan. 2007.

[22] F. R. Gfeller and U. Bapst, "Wireless in-house data communication via diffuse infrared radiation," *Proc. IEEE*, vol. 67, no. 11, pp. 1474–1486, Nov. 1979.

[23] H. Zhang and H. Dai, "Cochannel interference mi.ga.on and coopera.ve processing in downlink mul.cell mul.user MIMO networks," *EURASIP J. Wireless Commun. Netw.*, vol. 2004, no. 2, pp. 222–235, Dec. 2004.

[24] C.-S. Chang, "Stability, queue length, and delay of deterministic and stochastic queueing networks," *IEEE Trans. Autom. Control*, vol. 39, no. 5, pp. 913–931, May 1994.

[25] C.-S. Chang and J. A. Thomas, "Effective bandwidth in high-speed digital networks," *IEEE J. Sel. Areas Commun.*, vol. 13, no. 6, pp. 1091–1100, Aug. 1995.

[26] J. G. Kim and M. Krunz, "Bandwidth allocation in wireless networks with guaranteed packet-loss performance," *IEEE/ACM Trans. Netw.*, vol. 8, no. 3, pp. 337–349, Jun. 2000.

[27] J. Tang and X. Zhang, "Quality-of-service driven power and rate adaptation for multichannel communications over wireless links," *IEEE Trans. Wireless Commun.*, vol. 6, no. 12, pp. 4349–4360, Dec. 2007.

[28] D. P. Palomar and M. Chiang, "A tutorial on decomposition methods for network utility maximization," *IEEE J. Sel. Areas Commun.*, vol. 24, no. 8, pp. 1439–1451, Aug. 2006.
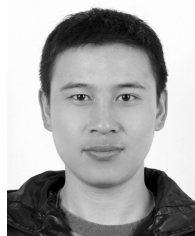
FAN JIN received the B.Eng. and M.Sc. degrees in electronics and information engineering from the Huazhong University of Science and Technology, Wuhan, China, in 2008 and 2010, respectively, and the Ph.D. degree in Southampton wireless from the School of Electronics and Computer Science, University of Southampton, Southampton, U.K, in 2015, which was funded by a scholarship under the U.K.-China Scholarships for Excellence Programme. His research interests include multiuser communications, radio resource allocation, spectrum sensing, and interference management in femtocells and heterogeneous networks. Since 2015, he has been with Huawei, Shenzhen, China.
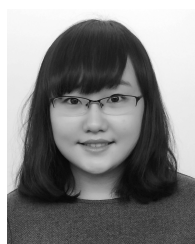
XUAN LI received the B.Eng. degree in optical information science and technology from the Beijing Institute of Technology, China. She is currently pursuing the Ph.D. degree with the Southampton Wireless Group, University of Southampton, U.K. Her research interests include visible light communications, heterogeneous networks, resource allocation, and scheduling algorithms.
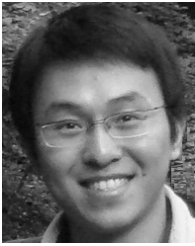
RONG ZHANG (M'09) received the Ph.D. degree from the University of Southampton, U.K., and the B.Sc. from Southeast University, China. He was an Engineer with China Telecom and a Research Assistant (2006-2009) with the Mobile Virtual Center of Excellence (MVCE), U.K. After being a Post-Doctoral Researcher (2009-2012) at the University of Southampton, he took industrial consulting leave (2012-2013) with Huawei Sweden R&D as a System Algorithms Specialist. Since 2013, he has been a Lecturer with the CSPC Group of ECS, University of Southampton. He has 40+ journals in prestigious publication avenues (e.g., the IEEE and OSA) and many more in major conference proceedings. He regularly serves as a Reviewer of the IEEE Transactions/journals and has been several times as a TPC Member/Invited Session Chair of major conferences. He is a recipient of joint funding of MVCE and EPSRC and is also a Visiting Researcher under Worldwide University Network.
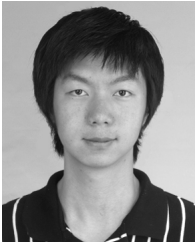
CHEN DONG received the B.S. degree in electronic information sciences and technology from the University of Science and Technology of China (USTC), Hefei, China, in 2004, the M.Eng. degree in pattern recognition and automatic equipment from the University of Chinese Academy of Sciences, Beijing, China, in 2007, and the Ph.D. degree from the University of Southampton, U.K., in 2014. He was a post-doc. In 2015, he joined Huawei, Shenzhen, China. His research interests include applied math, relay system, channel modeling, and cross-layer optimization. He was a recipient of scholarship under the U.K.-China Scholarships for Excellence program and the best paper award at the IEEE VTC 2014-Fall.

LAJOS HANZO (F'04) received the D.Sc. degree in electronics and the Ph.D. degree in 1976 and 1983, respectively, and the Doctor Honoris Causa degree from the Technical University of Budapest, in 2009. During his 40-year career in telecommunications, he has held various research and academic posts in Hungary, Germany, and the U.K. Since 1986, he has been with the School of Electronics and Computer Science, University of Southampton, U.K., where he holds the Chair in Telecommunications. He has successfully supervised over 100 Ph.D. students, co-authored 20 John Wiley/IEEE Press books on mobile radio communications totaling in excess of 10 000 pages, published 1550+ research entries at the IEEE Xplore, acted both as TPC and General Chair of the IEEE conferences, presented keynote lectures, and has been awarded a number of distinctions. He is currently directing a 100-strong academic research team, working on a range of research projects in the field of wireless multimedia communications sponsored by the industry, the Engineering and Physical Sciences Research Council (EPSRC), U.K., the European Research Council's Advanced Fellow Grant, and the Royal Society's Wolfson Research Merit Award. He is an Enthusiastic Supporter of industrial and academic liaison and he offers a range of industrial courses. He is also a Governor of the IEEE VTS. From 2008 to 2012, he was the Editor-in-Chief of the IEEE Press and a Chaired Professor with Tsinghua University, Beijing. His research is funded by the European Research Council's Senior Research Fellow Grant. He has over 24 000 citations. He is a fellow of IET and EURASIP.

• • •